Viscosimeter on a Microfluidic Chip

Pierre Guillot,* Pascal Panizza, Jean-Baptiste Salmon, Mathieu Joanicot, and Annie Colin

Rhodia Laboratoire du Futur, Unité Mixte Rhodia-CNRS, Université Bordeaux I, 178 Avenue du Docteur Schweitzer, 33608 Pessac, France

Charles-Henri Bruneau and Thierry Colin

MAB Université Bordeaux 1, CNRS UMR 5466, INRIA Futurs Projet MC2, 351 Cours de la Libération, 33405 Talence, France

Received January 13, 2006. In Final Form: April 12, 2006

In this work, a viscosimeter implemented on a microfluidic chip is presented. The physical principle of this system is to use laminar parallel flows in a microfluidic channel. The fluid to be studied flows side by side with a reference fluid of known viscosity. By using optical microscopy, the shape of the interface between both fluids can be determined. Knowing the flow rates of the two liquids and the geometrical features of the channel, the mean shear rate sustained by the fluid and its viscosity can thus be computed. Accurate and precise measurements of the viscosity as a function of the shear rate can be made using less than 300 μL of fluid. Several complex fluids are tested with viscosities ranging from 10^{-3} to 70 Pa·s.

I. Introduction

Complex fluids, such as foams or emulsions, are characterized by the existence of a mesoscopic length scale ranging from the molecular size to the whole sample.[1] For instance, in an emulsion, this characteristic size is that of a droplet. Because of such mesoscopic length scales, couplings between the structure of the complex fluid and the flow field may exist, leading to non-Newtonian behavior. Thus, stretching of solute polymer molecules in a shear flow induces a decrease in the fluid viscosity (and therefore shear thinning behavior) at high shear rates. Characterizing the response of a sample under flow therefore requires the determination of a rheological curve giving the evolution of the viscosity as a function of the applied shear rate. Rheological behaviors are key parameters in many fields, ranging from medicine and food processing to the chemical and manufacturing industries. In the food industry, the stability of dressings is often obtained by increasing the viscosity. However, the viscosity of a medication must be low enough to be infused using a needle and a syringe. The development of these products thus requires the use of additives that tune the viscosity of the product to the range required by the final application. The formulation of the appropriate additives in a mixture is tedious screening work that involves a series of long trials and tests. The use of through-put techniques in this field would both increase efficiency and reduce costs of research and development for the chemical industry. Microfluidics, which deals with the methods and materials needed to control and handle liquid flows on length scales ranging from tens to hundreds of micrometers, offers numerous prospects along these lines.[2] Microfluidic devices allow one to prepare samples of various compositions, which is the first step in the screening process, using very small volumes of fluids. Injecting two fluids at the inlet of a T junction and varying the ratio of the two flow rates allow one to obtain, in the outlet channel, mixtures of various compositions. However, to exploit the benefits of microfluidics, the development of new analytical tools on the micrometer length scale, such as rheological ones, is required. Miniaturized sliding plate rheometers have been fabricated to measure the steady shear viscosity of complex fluids using less than 10 μL of sample.[3−6] In such devices, the shear response of the sample is probed using a piezzoelectric-based method. Despite their performances, these systems remain difficult to operate because of the high precision required in the alignment of the two parallel plates. They must be separated from each other by less than 60 μm. Capillary viscosimeters are easier to miniaturize. Following this approach, Burns and co-workers[7] have developed a viscosimeter based on capillary pressure-driven flow inside microfluidic channels. A drop of liquid is placed at the inlet of a microchannel. The difference in the shape of the advancing and receding menisci causes a capillary pressure difference and propels the liquid down the channel. The measurement of the advancing speed of the liquid inside the channel yields the computation of the sample viscosity. Accurate measurements are achieved using only 600 nL of sample in less than 100 s. This low-cost method is well designed for biological liquids such as urine, blood, and blood plasma but remains limited to low-viscosity samples (less than 10^{-2} Pa·s). In a similar approach based on pressure-driven flow, Weng et al. have developed a viscosimeter equipped with a thermostat.[8] They measured the pressure drop and the flow rate of a liquid passing through a microtube. Recently, Kang and co-workers[9] measured the total pressure drop along a microchannel for an imposed flow rate using a pressure sensor. They measured the rheological properties of polymer solutions at high shear rates. The main drawback of their system is that it relies on the use of an external pressure transducer that measures the sum of the true microchannel pressure drop and those due to entrance and exit effects. To take these effects into account, both complex calibrations and corrections have to be applied. To avoid

* Corresponding author. E-mail: pierre.guillot-exterieur@eu.rhodia.com.

(1) Larson, R. G. *The Structure and the Rheology of Complex Fluids*; Oxford University Press: Oxford, England, 1999.
(2) Squires, T. M.; Quake, S. R. *Rev. Mod. Phys.* **2005**, *77*, 977.
(3) Hu, H.-W.; Granick, S. *Langmuir* **1994**, *10*, 3857.
(4) Granick, S.; Hu, H.-W.; Carson, G. A. *Langmuir* **1994**, *10*, 3867.
(5) Soga, I.; Dhinojwala, A.; Granick, S. *Langmuir* **1998**, *14*, 1156.
(6) Clasen, C.; McKinley, G. H. *J. Non-Newtonian Fluid Mech.* **2004**, *124*, 1.
(7) Srivastava, N.; Davenport, R. D.; Burns, M. A. *Anal. Chem.* **2005**, *77*, 383.
(8) Silber-Li, Z. H.; Tan, Y. P.; Weng, P. F. *Exp. Fluids* **2004**, *36*, 586.
(9) Kang, K.; Lee, L. J.; Koelling, K. W. *Exp. Fluids* **2005**, *38*, 222.

10.1021/la060131z CCC: $33.50
Published on Web 06/09/2006

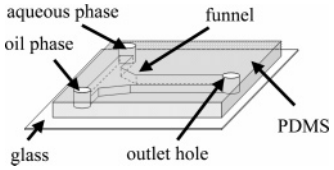

Figure 1. Sketch of our microfluidic device.

this type of correction, Galambos and co-workers[10] have proposed to use the features of specific microfluidic flows. After a T junction, two miscible fluids flowing side by side in the outlet channel are mixed by interdiffusion. Right after the T junction, the interface between the two fluids is still sharp because, under their experimental conditions, diffusion is slower than convection. In the channel, the position of the interface is fixed by the ratio of the flow rates of the two fluids and by the ratio of their viscosities. These authors show that by measuring the position of this interface using fluorescence microscopy they manage to compute the viscosity of one sample knowing the flow rates and the viscosity of the other fluid.

In our present work, we revisite their approach and extend it to complex fluids. The main originality of our work deals with the determination of the viscosity as a function of the shear rate. Using classical rheological procedures, we compute the mean shear rates sustained by the studied fluid and are consequently able to map the entire flow curve. The use of immiscible fluids gets rid of interdiffusion processes and allows us to measure the rheological behavior of the sample even for very low shear rates. In the following text, we present the physical principles of our system. The second part deals with the precision of the experiments, whereas the third part is devoted to the materials and methods used. The experimental results are finally presented and discussed in the fourth part of this article.

II. Principle of the Microviscosimeter

Following the work of Galambos[10] and Groisman,[11,12] we use an optical tool to measure the pressure drop in a microchannel. Our microdevices have two inlet arms that meet at a T junction (Figure 1). They are made with standard soft lithography methods (Methods section) using polydimethylsiloxane (PDMS) and glass.[13] As depicted in Figure 1, three of the channel walls are made of PDMS, and the last one is made of glass. The two inlet arms are filled with two immiscible fluids (typically an oil phase and an aqueous phase).

When these two immiscible fluids reach the T junction, depending on the flow rates of the two fluids, various flow patterns (droplets, unstable parallel flow, or parallel flow) are observed in the outlet channel. Figure 2 displays some typical microscopy pictures obtained under various conditions. In a wide range of flow rates, the two immiscible fluids flow side by side, forming a laminar parallel flow (PF).[2,14−16] By measuring the position of the interface between these two fluids and by knowing the flow rates of both fluids and the viscosity of one of them, the viscosity of the other fluid and the pressure drop in the microchannel can be computed. However, to do so precisely, the exact shape of the interface between both fluids is required to model and compute the flow field.

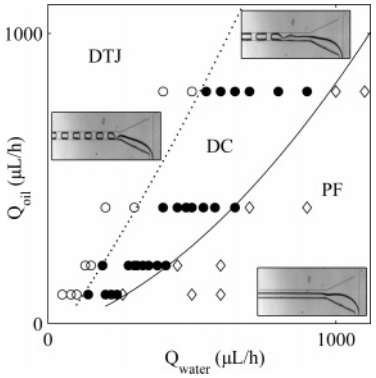

Figure 2. Flow pattern diagram as a function of the aqueous-phase flow rate (Q_{water}) and of the oil-phase flow rate (Q_{oil}) in a 100 μm × 100 μm microchannel. The aqueous phase is a mixture of water with 50 wt % sodium dodecyl sulfate (SDS) (2 cmc) and 50 wt % glycerine. The oil phase is hexadecane. The open circles (○) refer to droplets formed at the T junction (DTJ); the open squares (□), to parallel flows (PF); and the solid circles (●), to parallel flows that break into droplets inside the channel (DC).

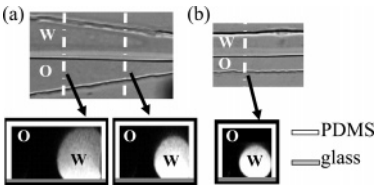

Figure 3. Cross-sectional picture of the parallel flow between hexadecane (O) and the aqueous phase with rhodamine (W) in a 100 μm × 100 μm microchannel. (a) Inside the funnel. (b) In the outlet channel.

A. Shape of the Free Fluid−Fluid Interface. To investigate the three-dimensional structure of the flow, confocal fluorescence microscopy experiments are performed. In this case, a small amount of rhodamine is added to the aqueous phase, and hexadecane is used as the oil phase.

Figure 3 displays cross-section images obtained for PF in a 100 μm × 100 μm microchannel. The channel walls represented here have been drawn and added to the picture. The bottom wall is made of glass, and the three others are made of PDMS. Figure 3 shows the establishment of the flow after the T junction. Two steps can be distinguished. In the first one, at the entrance of the funnel, hexadecane starts to wrap around the water by the PDMS wall. This is due to the difference in wettability of the two fluids with the PDMS walls. The cross section of the water stream evolves until it reaches a shape with a single radius of curvature. Downstream from this point, the pressure drop across the interface between the two fluids remains constant. Because the interface does not move from this point, the pressure is constant in each fluid in a cross section of the channel (i.e., the velocity component in the cross section is null). The single-curvature radius shape of the free liquid−liquid interface is thus a signature of unidirectional flow.

In a 200 μm × 100 μm microchannel (Figure 4) or for higher water flow rates in a 100 μm × 100 μm microchannel, the behavior of the flow is the same: the interface reaches a single-curvature shape. However, the shape of the free liquid−liquid interface is slightly different. The water phase is in contact with the two walls and is not completely wrapped by the oil phase. The contact angles on the PDMS and on the glass are different because of the difference in affinity between the oil and the two solid (PDMS or glass) plates. This contact angle seems to vary at high flow

(10) Galambos, P.; Forster, F. *Int. Mech. Eng. Congr. Exp.*, Anaheim, CA 1998.
(11) Groisman, A.; Enzelberg, M.; Quake, S. R. *Science* **2003**, *300 9*, 955.
(12) Groisman, A.; Quake, S. R. *Phys. Rev. Lett.* **2004**, *92*, 094501.
(13) Duffy, D. C.; McDonald, J. C.; Schueller, O. J. A.; Whitesides, G. M. *Anal. Chem.* **1998**, *70*, 4974.
(14) Thorsen, T.; Roberts, R. W.; Arnold, F. H.; Quake, S. R. *Phys. Rev. Lett.* **2001**, *86*, 4163.
(15) Tice, J. D.; Lyon, A. D.; Ismagilov, R. *Anal. Chim. Acta* **2004**, *507*, 73.
(16) Guillot, P.; Colin, A. *Phys. Rev. E* **2005**, *72*, 066301.

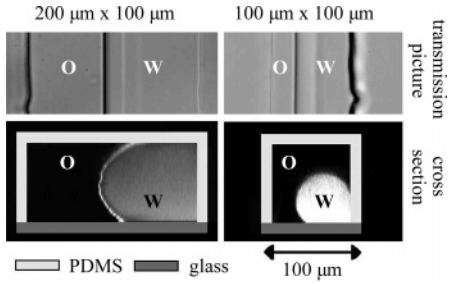

Figure 4. Cross-sectional picture of the parallel flow between hexadecane (O) and the aqueous phase with rhodamine (W) in a 200 μm × 100 μm and a 100 μm × 100 μm microchannel.

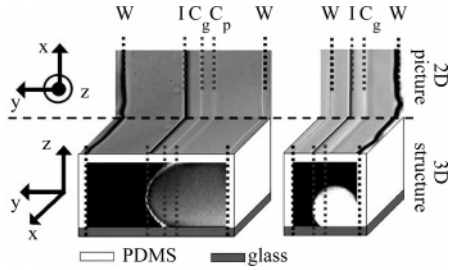

Figure 5. Analysis of the transmission picture obtained with a 200 μm × 100 μm and a 100 μm × 100 μm microchannel. Transmission pictures are a projection of the 3D structure of the flow. They contain different lines (referred to below as W, I, C_p, and C_g) that allow us to access structural information on the shape of the interface between both fluids. W represents the PDMS walls, C_p and C_g are the contact lines on PDMS and glass, respectively, and I corresponds to the maximum length of the water phase in the *y* direction. Because the shape of the interface must be circular, it is thus possible to reconstruct the 3D structure of the flow with only a single transmission picture.

rates. We believe that there are nontrivial dynamical issues due to the gradient of velocity in the *z* direction of the flowing liquids. This evolution is measured and taken into account in the determination of the free fluid−fluid interface.

Note that the shape of the interface can also be revealed by optical microscopy pictures as shown in Figure 5. The mismatched lines correspond to the PDMS walls (W), to the interface position (I), and to the contact lines on the glass plate (C_g) or on the PDMS surface (C_p). Knowing the position of these lines and the position of the interface between the two flowing fluids and assuming that the interface is a part of a cylindar, the radius of the interface and the position of its center can be obtained numerically.

From this information, the velocity field can be computed, and the viscosity and the mean shear rate sustained by the fluid sample can be deduced using the procedure described in the following section.

B. Description of the Flow Field for Newtonian Fluids. Assuming that the steady state is reached and that both fluids are Newtonian and incompressible, we write the conservation of matter equation:

$$\mathbf{div}\ \vec{v}_i = 0 \tag{1}$$

and the Stokes equation for both fluids:

$$\eta_i \Delta \vec{v}_i = \mathbf{g\vec{r}ad}\ P_i \text{[17]} \tag{2}$$

where $\vec{v}_i$, η_i, and P_i are the velocity vector, the viscosity, and the pressure inside the fluid *i*, respectively. *i* equals either 1 or 2, where $i = 1$ stands for the oil phase and $i = 2$ stands for the aqueous phase. In a parallel flow, the flow is unidirectionnal. If

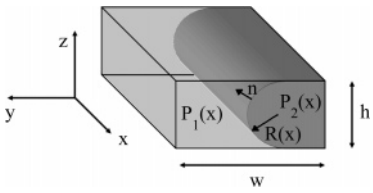

Figure 6. Notation used.

x is the mean axis of the channel (Figure 6), then the velocity field can be written as:

$$\vec{v}_i = u_i(x, y, z)\vec{e}_x \tag{3}$$

Equations 2 and 3 imply that the pressure in each fluid is a function of *x* only and is constant in cross section. The pressures in both fluids are linked by the Laplace law through:

$$P_2(x) - P_1(x) = \frac{\gamma}{R(x)} \tag{4}$$

where γ is the surface tension and $R(x)$ is the radius of the interface. Because $R(x)$ is constant all along the channel in a parallel flow, the pressure gradients in both fluids are equal:

$$\frac{\partial P_1}{\partial x} = \frac{\partial P_2}{\partial x} \tag{5}$$

The incompressibility of the flow implies that the velocity does not depend on *x* and that the pressure gradient is a linear function of *x*. Using eq 3, eq 2 becomes eq 6, and eq 1 is satisfied:

$$\eta_i \Delta u_i = \frac{P_{\text{entrance}} - P_{\text{exit}}}{L} = \frac{\delta P}{L} \tag{6}$$

where *L* is the length of the channel.

This set of equations is closed by defining the boundary conditions, namely, that the velocity and the tangential components of the stress tensor are continuous at the interface and there is no slip at the walls for either fluid.[18,19] At the wall, the no-slip boundary condition implies that:

$$u_i = 0 \tag{7}$$

whereas the continuity of the velocity and of the shear stress at the fluid−fluid interface leads to:

$$u_1 = u_2 \qquad \text{and} \qquad \eta_1 \frac{\partial u_1}{\partial n} = \eta_2 \frac{\partial u_2}{\partial n} + \eta_s \frac{\partial^2 u_2}{\partial^2 t} \tag{8}$$

where *n*, *t*, and η_s respectively stand for the normal vector to the interface oriented from fluid 2 to fluid 1, the tangent vector of the interface perpendicular to *x*, and the interface shear viscosity, respectively. For surfactant monolayers at the oil−water interface, typical values of η_s range from 10^{-9} to 10^{-7} Pa·s·m. In the case of a 100 μm × 100 μm channel, the viscosity surface term is negligible for fluid viscosities higher than:

$$\eta > \frac{\eta_s}{l} \simeq 10^{-3}\ \text{Pa·s} \tag{9}$$

(17) This notation is not the Einstein notation.

(18) Guyon, E.; Hulin, J.-P.; Petit, L.; Mitescu, C. D. *Physical Hydrodynamics*; Oxford University Press: Oxford, England, 2001.

(19) Bird, R. B.; Stewart, W. E.; Lightfoot, E. N. *Transport Phenomena*, 2nd ed.; Wiley: New York, 2002.

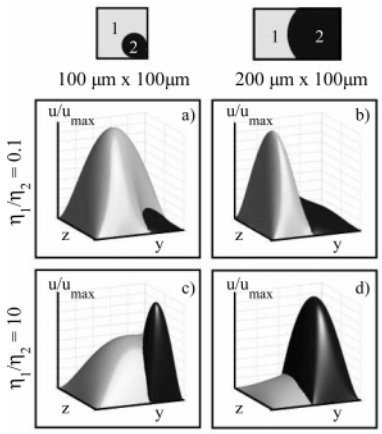

Figure 7. Velocity profiles of two immiscible fluids in a 100 μm $\times$ 100 μm and a 200 μm $\times$ 100 μm microchannel. Profiles are made for two viscosity ratio. Fluid 1 corresponds to the oil phase, and fluid 2, to the aqueous phase.

Consequently, in the following text we will neglect this term. Knowing the viscosity of both fluids, the pressure gradient, and the shape of the interface, this set of equations allows us to compute the flow rate of each fluid according to:

$$Q_i = \int_0^w \int_0^h u_i(y, z)\, dy\, dz \tag{10}$$

A dimensional analysis of this set of equations points out that, for a given shape and position of the interface, the ratio of the two flow rates must depend only on the ratio between the two fluid viscosities. Note that the pressure drop along the flow direction only sets the exact values of the flow rates but does not fix their ratio. In other words, the interface between the two Newtonian fluids does not move when the two corresponding flow rates are increased or decreased while keeping their ratio constant as shown in Figure 15.

C. Numerical Procedure. To perform numerical simulations, we introduce a global function u defined over the whole domain Ω by $u = u_i$ on Ω_i. We also need a global viscosity $\eta = \eta_i$ on Ω_i. Ω is the cross section of the channel, Ω_i is the cross section of the aqueous $i = 2$ or of the oil stream $i = 1$. Equation 6 and the continuity of the velocity at the interface imply that the functions u and η satisfy eq 11:

$$\nabla(\eta \nabla u) = \frac{\delta P}{L} \tag{11}$$

in the domain Ω. The velocity u vanishes at the boundary of Ω. Note that the interface does not appear anymore in this formulation. It is present only through the value of the function η, which is discontinuous. Independent of the shape of this interface, we use a Cartesian regular mesh. We use a finite volume discretization of the equations that ensures the continuity of the fluxes at the interface.[20] The computations are done using the scientific software Scilab developed by INRIA. Figure 7 shows the typical flow profiles obtained over areas of 100 μm $\times$ 100 μm and 200 μm $\times$ 100 μm for two viscosity ratios.

When fluid 1 is less viscous than fluid 2 (Figure 7a and b), the velocity field of fluid 2 ressembles a shear flow and a homogeneous shear stress can be defined. This is not the case when fluid 1 is more viscous. The flow field of fluid 2 in Figure 7c and d resembles a poiseuille flow in which the shear stress is heterogeneous. To get a well-defined shear stress in our experiments dealing with non-Newtonian fluids, we will thus use a low-viscosity fluid as a reference fluid.

(20) Eymard, R.; Gallouët, T.; Herbin, R. *Finite Volume Methods Handbook of Numerical Analysis* (Ciarlet, P. G.; Lions, J. L. 2000).

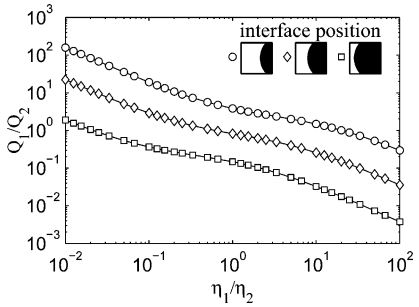

Figure 8. Flow rate ratio Q_1/Q_2 as a function of the viscosity ratio η_1/η_2 for three positions of the interface. The channel dimensions are 100 μm $\times$ 100 μm.

D. Determination of the Viscosity of Newtonian Fluids. In the calculations previously detailed, we set the viscosity of the two fluids, the position of the interface, the pressure gradient, and we compute the flow rates. However, in our experiments, we impose the two flow rates, we measure the position and the shape of the interface, and we know only the viscosity of one of the two fluids. Solving this inverse problem for a given shape and flow rate ratio allows us to find the corresponding viscosity ratio and, thus, to find the unknown viscosity. Figure 8 shows the evolution of the flow rate ratio as a function of the viscosity ratio for various positions of the interface. Because this curve is bijective, the experimental flow rate ratio clearly sets the value of the viscosity ratio.

To converge toward the correct viscosity ratio, we solve the equation $Q_1/Q_2 = f(\eta_1/\eta_2)$ numerically where the function f is calculated as previously described. An arbitrary viscosity ratio is fixed, and the corresponding flow rate ratio $(Q_1/Q_2)_c$ is computed and compared to the experimental ratio using the relation:

$$\frac{Q_1/Q_2 - (Q_1/Q_2)_c}{Q_1/Q_2} = \Delta q \tag{12}$$

This procedure is stopped when Δq becomes less than 10^{-3}. We choose to stop the procedure at 10^{-3} because the numerical error made in the determination of the viscosity ratio is much lower than the experimental one discussed below. The entire flow profile in the channel and the mean shear rate $\dot{\gamma}$ sustained by the sample (the mean value of the norm of the velocity gradient) can then be computed according to:

$$||\mathbf{grad}\, u|| = \sqrt{\left(\frac{\partial u}{\partial y}\right)^2 + \left(\frac{\partial u}{\partial z}\right)^2} \tag{13}$$

$$\dot{\gamma} = \frac{1}{S}\int_0^w \int_0^h ||\mathbf{grad}\, u||\, dy\, dz \tag{14}$$

where S is the surface of a cross section filled with the sample.

A standard deviation $\Delta\dot{\gamma}$ defined below is associated with this mean value:

$$\Delta\dot{\gamma} = \frac{1}{S}\int_0^w \int_0^h \sqrt{||(\mathbf{grad}\, u||^2 - \dot{\gamma}^2)}\, dy\, dz \tag{15}$$

E. Determination of the Viscosity of Non-Newtonian Fluids. The above calculation allows us to measure the viscosity of a Newtonian fluid. To extract the flow curve for a non-Newtonian fluid, we follow the procedure used in classical rheometry. Let us first recall, briefly, how these measurements are performed for rotational rheometers using a Couette cell. With such a cell

geometry, the sample is sandwiched between two coaxial cylinders of radius R_1 and R_2. One cylinder is fixed while the other one, connected to a rotation axis, is free to rotate. The experiment is then performed in the following way: a motor applies a torque Γ to the rotation axis, and the rotation speed of the axis ω is recorded. In this cylindrical geometry, the shear stress σ and the shear rate $\dot{\gamma}$ endured by the sample are not constant. They vary as a function of the distance r to the rotation axis.

To extract the viscosity of the sample from the two measured quantities Γ and ω, mean values of the shear rate $\langle\dot{\gamma}\rangle$ and of the shear stress $\langle\sigma\rangle$ are defined.[18] These engineering values are related to the torque applied to the axis and to the rotation speed as follows:

$$\langle\sigma\rangle = \frac{\sigma(R_1) + \sigma(R_2)}{2} = \frac{{R_1}^2 + {R_2}^2}{4\pi H {R_1}^2 {R_2}^2}\Gamma \qquad (16)$$

$$\langle\dot{\gamma}\rangle = \frac{\dot{\gamma}(R_1) + \dot{\gamma}(R_2)}{2} = \frac{{R_1}^2 + {R_2}^2}{{R_2}^2 - {R_1}^2}\omega \qquad (17)$$

The viscosity of the sample is given by $\langle\sigma\rangle/\langle\dot{\gamma}\rangle$. However, these relationships are exact only for a Newtonian fluid subjected to a steady flow in the absence of slip at the wall. For non-Newtonian fluids, the flow curve extracted from the measurement corresponds, therefore, to the shear rate and the shear stress of a Newtonian fluid under the same experimental conditions.

In our present work, we will use a similar procedure to extract the flow curve from our experiments. We will associate with the non-Newtonian fluid the viscosity and the mean shear rate that a Newtonian fluid would have under the same experimental conditions (same flow rates and same viscosity of the standard fluid).

III. Precision of the Measurements

Let us now discuss the precision range obtained for the measurements of the shear rate and the viscosity and point out the required experimental conditions to enhance the accuracy of the measurement. Two causes of uncertainty have to be pointed out. First, the flow in the microchannel is not a pure shear flow. The shear rate varies as a function of the position in the cross section of the microchannel, inducing deviations in the value of $\dot{\gamma}$ that are inherent to the method. We will quantify these deviations and discuss how they are influenced by the geometry of the microchannel and by the viscosity ratio. Second, the accuracy of the viscosity measurement is affected by the error bars on the experimental parameters. We will therefore estimate the errors made in the measurement of the flow curve due to the experimental uncertainties in the optical determination of the interface position. Note that syringe pumps allow us to control the flow rates with a precision of 0.35%.[21] This uncertainty is much lower than the two others mentioned before and will not be discussed below.

A. Precision of the Measured Shear Rate. To estimate the accuracy of the shear rate, we compute the standard deviation of a Newtonian fluid for various experimental conditions. The calculations have been made for the aqueous phase, which corresponds to fluid 2 in our previous notation. Figure 9 presents the standard deviation of the shear rate divided by the mean shear rate for fluid 2 in a 100 μm × 200 μm microchannel. Curves display the deviation obtained for different viscosity ratios as a function of $(Q_1/Q_2)(\eta_1/\eta_2)$.

(21) Harvard Apparatus; *PHD 22/2000 Syringe Pump Series User's Manual*.

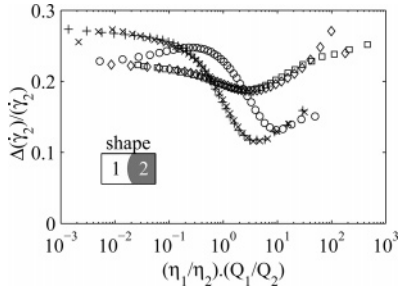

Figure 9. Standard deviation of the mean shear rate of fluid 2 divided by the mean shear rate as a function of $(Q_1/Q_2)(\eta_1/\eta_2)$. Microchannel dimensions are 200 μm × 100 μm. This deviation is calculated for different viscosity ratios η_1/η_2. + corresponds-to-a ratio of 0.01; ×, to a ratio of 0.1; ○, to a ratio of 1; □, to a ratio of 10; and ◇, to a ratio of 100.

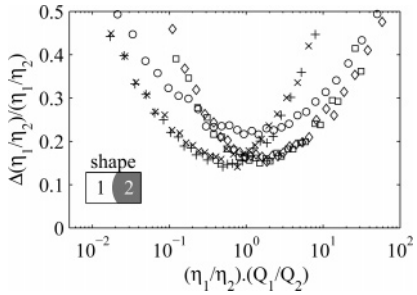

Figure 10. Error in the viscosity ratio due to an imprecision of ±5 μm in the localization of the different lines. The channel dimensions are 200 μm × 100 μm. This error is computed for different Q_1/Q_2 ratios. + corresponds to a ratio of 0.01; ×, to a ratio of 0.1; ○, to a ratio of 1; □, to a ratio of 10; and ◇, to a ratio of 100.

The shape of the interface is presented in the inset of the Figure. As previously discussed, it is a one-radius-curvature surface with a curvature radius of $R = 2h$, where h is the height of the channel. Figure 9 clearly shows that best accuracy (less than 15%) is reached when η_1/η_2 is equal to 0.1 (×) or 0.01 (+). This is when the oil phase is less viscous than the aqueous phase. Under those conditions, the most homogeneous shear rates are obtained when $Q_1/Q_2 = 3/(\eta_1/\eta_2)$. The flow field inside the sample resembles a shear flow. This corresponds to flow profile b in Figure 7.

Note that this behavior is not affected by the dimensions of the channel. Similar conclusions are reached in a 100 μm × 100 μm microchannel. A low viscosity ratio and a high flow rate ratio seem to be the key parameters needed to obtain a high measurement precision.

B. Experimental Restrictions. When we take the transmission picture and analyze the characteristic lines, there is imprecision in determining the position of the PDMS walls, the interface between the two fluids, and the contact lines. This imprecision arises mainly from the roughness of the PDMS walls. Swelling of the PDMS channels or bending of the walls under high driven pressure may also contribute to these uncertainties. However, these deformations seem to be very low in our experiments. This problem in the detection may induce an error in the determination of the viscosity. We estimate this imprecision to be ±5 μm. To study the effect of this experimental incertitude, we fix one flow rate ratio and the position of the interface and calculate the viscosity ratio η_1/η_2. We do exactly the same for an interface located at +5 μm and at −5 μm. The difference between the two viscosity ratios obtained at ± 5 μm gives the error in the viscosity ratio $\Delta(\eta_1/\eta_2)$. Figure 10 presents the evolution of the error of the viscosity ratio for five Q_1/Q_2 values as a function of $(Q_1/Q_2)(\eta_1/\eta_2)$ for a 100 μm × 200 μm channel. This Figure shows

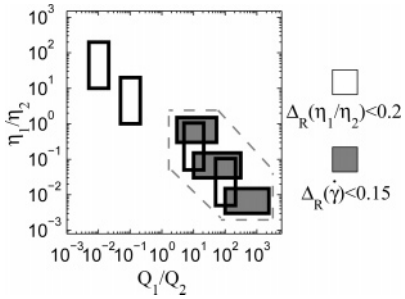

Figure 11. Domain where the viscosity (□) and the shear rate (■) are well defined in a 200 μm × 100 μm microchannel. The area where rheological measurements can be made with the best accuracy is shown in the graph.

that, to limit the error in the viscosity ratio, the flow rate ratio between the two fluids has to be different from 1. It appears clearly that, for other viscosity ratios, there exists a range of flow rate ratios that allows a precision lower than 0.2 to be reached. Similar conclusions are reached in a 100 μm × 100 μm microchannel.

Figure 11 sums up the different results. Couples of (Q_1/Q_2, η_1/η_2) that satisfy $\Delta(\eta_1/\eta_2)/(\eta_1/\eta_2) \leq 0.2$ (rectangle in Figure 11) or $\Delta(\dot{\gamma})/(\dot{\gamma}) \leq 0.15$ (plain rectangle in Figure 11) are shown on the graph. It appears to be an area where the most accurate rheological measurements can be made.

In conclusion, to determine the viscosity of a fluid with our microviscosimeter accurately, it is better to work with two fluids with viscosity ratios higher than 10 or lower than 0.1. Our experiments required precise determinations of both the viscosity and the shear rate. We will thus choose a less viscous reference fluid and use only a viscosity ratio between the sample and the reference fluid higher than 10.

IV. Materials and Methods

A. Materials. In this work, various simple and complex fluids have been used. The Newtonian fluids are silicone oils of different viscosities, hexadecane, 1-octanol, dodecanol, glycerine, and dilute solutions of sodium dodecyl sulfate (SDS) above the critical micellar concentration (cmc) in water (cmc = 0.24 wt %). Various non-Newtonian solutions have been studied, including dilute solutions of polymers and surfactants in water and two different emulsions. The dilute solutions of polymers used are polyethyleneoxide (PEO) with a molecular weight of 4 000 000 (4M) at 1 and 2 wt % in water and polyacrylamide (PAA) with a molecular weight of 18M at 0.1 wt % in water. The first emulsion is a homemade emulsion. We have dispersed a silicone oil of high viscosity (η = 30 Pa·s) in an 8 wt % solution of trimethyl tetradecyl ammonium bromide (TTAB) in water. This emulsion has a characteristic size of 3 μm, and the oil volume fraction is 60%.[22] The second sample is a commercial mayonnaise (Amora, France). The surfactant solution is a mixture made of cetylpyridinium chloride (CpCl) and sodium salicylate (NaSal) diluted to 6 wt % in a solution of NaCl at 0.5 mol/L in water. This system is known to form wormlike micelles.[23,24]

B. Methods. Most of our microfluidic devices are fabricated using soft lithography technologies.[13] A mold is obtained by patterning an Su-8 photoresist (Microchem) on a silicon wafer by standard photolithography. Polydimethylsiloxane (PDMS) (Sylgard 184, Dow Corning) is cast on the mold and cured at 65 °C for 1 h. The channels are sealed with a glass plate after an oxidation step in an UV cleaner (Jelight). The microchannels thus have three walls in PDMS and one in glass. The channel dimensions are measured with a profilometer (Dektak 6M, Veeco); the heights vary from 50 to 100 μm, and the widths vary from 50 to 200 μm. The microdevices used in our experiments have two inlet arms that meet at a T junction with a funnel design. The use of a funnel allows us to reduce the droplet formation domain.

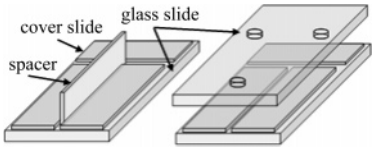

Figure 12. Method used to get a rectangular glass channel. Three cover slides are glued to a first slide with an optical adhesive to form a T junction. A spacer is used to ensure a constant width in the outlet channel. Access holes are made in another glass slide by sand blasting. The channel is then sealed by this glass slide with an optical adhesive.

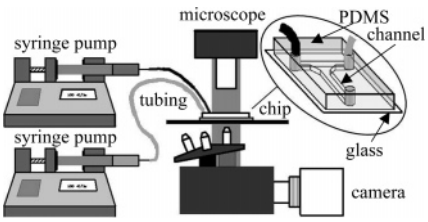

Figure 13. Setup used for our experiments. Two syringe pumps inject the two fluids into the microfluidic chip. PF are observed with an optical microscope. Pictures are recorded with a CCD camera.

Another kind of device has been fabricated to obtain rectangular glass channels. Three cover slides (200 μm thick) are glued to the first glass slide with an optical adhesive (NOA 81, Norland Products) to form a T junction. A spacer allows us to control the width of the outlet channel. Access holes are made in a second glass slide with a sand blaster. The channels are then sealed by this glass slide using the same optical adhesive. To clog the holes that appear on the edge, an optical adhesive droplet is placed on each hole. The distance between the two glass walls is measured under a microscope to get the real dimension of the channel.

The inlet channels are connected via tubing to syringes loaded with the fluids. Syringe pumps (PHD 2000, Harvard apparatus) allow us to control the flow rates of the liquids between 1 μL/h and 60 mL/h (Figure 13). To compare our measurements with classical ones, we performed rheological measurements of our solutions in a cone plate rheometer (AR 2000N, TA instruments) with a 4 cm diameter and a 2° angle cone cell.

V. Results and Discussion

In this section, we present our results obtained on Newtonian and non-Newtonian fluids with our microfluidic device. Error bars on viscosity and on the shear rate are calculated as previously discussed and are plotted with a cross of which the relative size depends on the calculated error for the two values. The results are compared with classical measurements.

A. Newtonian Fluids. Figure 14 presents the evolution of the position of the interface for various flow rates. Clearly, the oil phase grows when the oil flow rate is increased.

Figure 15 shows that the position of the interface between the two fluids does not move when the flow rates are increased while the ratio between them is kept constant. As previously discussed, such behavior proves that the two fluids are Newtonian. From these pictures, we extract the position of the interfaces between the oil and the SDS solution on the glass (C_g), on the PDMS (C_p), and in the bulk (I).

Figure 16 presents the viscosity measurement obtained on hexadecane. The measurements are performed at 22 °C. The shear stress varies linearly with the shear rate, thus hexadecane is a Newtonian fluid. The viscosity of hexadecane is found to be equal to 2.6 mPa·s and is in good agreement with the value found in the literature.[25]

(22) Salmon, J.-B.; Bécu, L.; Manneville, S.; Colin, A. *Eur. Phys. J. E* **2003**, *10*, 209.
(23) Berret, J.-F.; Roux, D. C.; Porte, G. *J. Phys. II* **1994**, *4*, 1261.
(24) Berret, J.-F.; Porte, G.; Decruppe, J.-P. *Phys. Rev. E* **1997**, *55*, 1668.

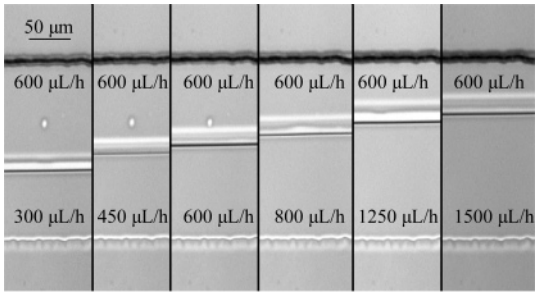

Figure 14. Optical pictures of the parallel flow measured for various flow rate ratios in a 200 μm × 100 μm microchannel. The oil phase is hexadecane. The aqueous phase is a solution of SDS in water at the cmc and is located in the upper part of the figure. The flow rates of water and hexadecane are specified. Note that the interface between the two fluids moves toward the upper part when the oil flow rate is increased.

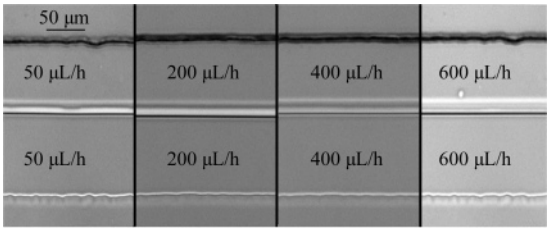

Figure 15. Optical pictures of the parallel flow taken for a fixed ratio between the flow rates in a 200 μm × 100 μm microchannel. The oil phase is hexadecane. The aqueous phase is a solution of SDS in water at the cmc and is located in the upper part of the figure. The flow rates of water and hexadecane are specified. The interface between the two fluids does not move for the different flow rates, which is proof of the Newtonian behavior of the two fluids.

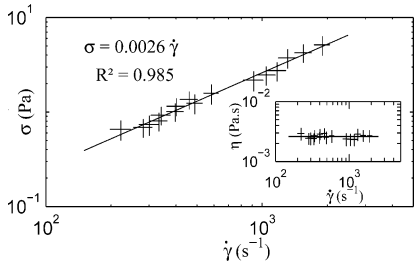

Figure 16. Flow curve of hexadecane. Shear stress varies linearly with shear rate. An inset displays the viscosity versus shear rate. The value obtained for viscosity is 2.6 mPa·s. The channel is a 100 μm × 100 μm glass PDMS channel, and water with SDS at the cmc (1 mPa·s) is used as the reference fluid.

Table 1 reports the values obtained for various fluids. In each case, the measured values are in good agreement with those found in the literature.[25]

B. Non-Newtonian Fluids. *Polymers.* Figure 17 presents the rheological curve obtained for PEO solutions of various concentrations. The measurements are performed at 22 °C. The data obtained with the microviscosimeter (+) are in very good agreement with the measurements performed on a classical cone plate rheometer (○ and ●). During this experiment, less than 250 μL of the fluids are injected into the system.

Similar conclusions are reached using 200 μL of PAA polymer solutions (Figure 18).

This data points out that we are able to measure the rheological behavior of the samples. Slip does not seem to occur or is sufficiently small so as not to affect our measurements. Numerical computations show that a slip length of 5% of the channel width is required to alter the measurement significantly.

Table 1. Results Obtained with Newtonian Fluids[a]

reference fluid	water	silicone oil	silicone oil	water
η/mPa·s	1	500	20	1
unknown fluid	1-octanol	glycerine	dodecane	hexadecane
η measured/mPa·s	9.3	860	1.2	2.6
η^{25}/mPa·s	8.5	890	1.3	3

[a] Values obtained with less than 20% experimental error are clearly in good agrement with the reference values found in the Handbook.[25] The accuracy of the Handbook values ranges from 1% (best case) to 10% (worst case).[25]

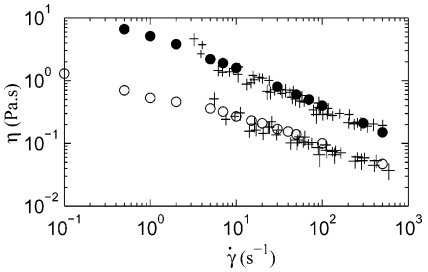

Figure 17. Viscosity as a function of shear rate for PEO 4M in water at 22 °C. ○ and ● represent the flow curves for PEO solutions at 1 and 2 wt % obtained with a cone plate rheometer. + represents the results with error bars obtained for the same solutions with our microviscosimeter. The channel is a 200 μm × 100 μm glass PDMS channel, and silicone oil at 0.1 Pa·s is used as the reference fluid.

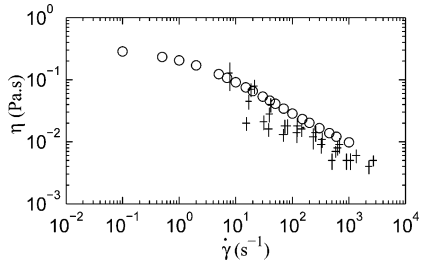

Figure 18. Viscosity as a function of shear rate for PAA at 0.1 wt % in water at 22 °C. ○ represents results obtained with a cone plate rheometer. + represent the results with error bars obtained for the same solution with our microviscometer. The channel is a 200 μm × 100 μm glass PDMS channel, and silicone oil at 20 mPa·s is used as the reference fluid.

Emulsions. Figure 19 presents the rheological curves obtained for the two different emulsions. The first sample is the homemade emulsion (◆), and the second sample is the commercial mayonnaise (●).

At first sight, the data obtained with our microviscosimeter are not in good agreement with the measurements performed on a classical rheometer (◆, ●, and +). Values found with the microviscosimeter are systematically lower than those obtained with a cone plate rheometer for any shear rate. However, the rheological response of these samples is very sensitive to preshear. Preshearing these emulsions in the cone plate at 1500 s^{-1} for 1 min leads to another flow curve (◇ and ○) that is in much better agreement with the measurements performed on our microviscosimeter. This means that the samples have been sheared before being injected into the microfluidic chip. We believe that this occurs during the manual loading of the tubing. In the future, we plan to design similar tanks to those of Ismagilov et al.[26] at the entrance of the microviscosimeter device in order to load the

(25) Lide, D. R., Ed.; *CRC Handbook of Chemistry and Physics*, 85th ed.; CRC Press: Boca Raton, FL, 2004; pp 6−203.

(26) Zheng, B.; Roach, L. S.; Ismagilov, R. F. *J. Am. Chem. Soc.* **2003**, 125, 11170.

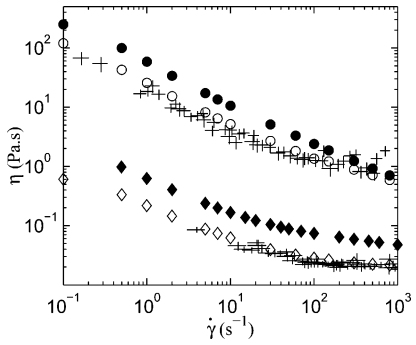

Figure 19. Viscosity as a function of shear rate. Homemade emulsion and mayonnaise at 22 °C. ◆ and ● represent the results obtained with a cone plate rheometer. + represents the results and error bars obtained for the same solution with the microviscosimeter. The results are not in good agreement, but they become much better when the solution is sheared prior to the measurement (◇ and ○). The channel is a 200 μm × 100 μm glass PDMS channel; silicone oil at 20 mPa·s is used as the reference fluid for the homemade emulsion, and silicone oil at 0.5 Pa·s is used as the reference fluid for the mayonnaise.

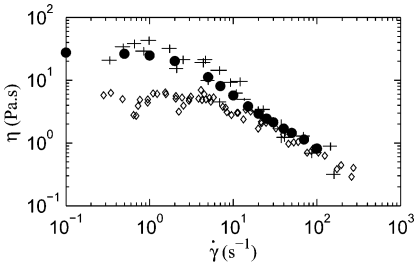

Figure 20. Viscosity as a function of shear rate for a solution made of 6% CpCl−NaSal in brine water at 22 °C. ◇ represents results obtained in a 200 μm × 100 μm glass PDMS channel. This is not in good agreement with cone plate rheometer mesurements (●) at low shear rates. Slip effects on PDMS are at the origin of this deviation. The results are in good agreement when we used a 300 μm × 200 μm glass channel (+) where no significant slip occurs. In both cases, silicone oil at 0.1 Pa·s is used as the reference fluid.

sample more gently and therefore avoid important and long-time preshearing of the sample. Note that viscosities as high as 70 Pa·s have been measured with our method.

Surfactants. Figure 20 presents the rheological curve obtained for the surfactant blend of CpCl and NaSal. This fluid is structured in wormilke micelles at the concentration used in this study.

The first measurements, performed in a 200 μm × 100 μm glass PDMS channel (◇ in Figure 20), are not in good agreement at low shear rates with the results obtained in a cone plate rheometer (● in Figure 20). This is not the case at high shear rates, where microviscosimeter data are similar to the rheometer measurements. This means that the error does not have the same origin as the one observed with the two emulsions. The fact that the effects are more important at low shear rates (i.e., low velocity) is compatible with slip arguments.[27,28] Crude particule imaging velocimetry (PIV) experiments have confirmed this hypothesis and have shown that slip essentially occurs at the PDMS walls and not on the glass surface (Figure 21).

To limit this problem, we have made the measurement in a 300 μm × 200 μm glass channel. The results obtained in this microdevice (+ in Figure 20) are in good agreement with cone

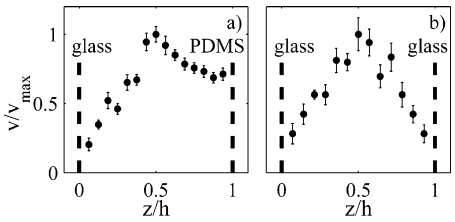

Figure 21. PIV measurements in a solution made of 6% CpCl−NaSal (a) in a 200 μm × 100 μm glass PDMS and (b) in a 300 μm × 200 μm glass channel. The curves represent the velocity in function of the z position at a fixed (x, y) position. In both cases, silicone oil at 0.1 Pa·s is used as the reference fluid. In the glass PDMS device, the CpCl−NaSal flow rate is 4 μL/h, the silicone oil flow rate is 40 μL/h, and we find $\dot{\gamma} = 2.2$ s^{-1} and $\eta = 5.3$ Pa·s. In the glass device, the CpCl−NaSal flow rate is 2 μL/h, the silicone oil flow rate is 100 μL/h, and we calculate $\dot{\gamma} = 0.5$ s^{-1} and $\eta = 20.6$ Pa·s. PDMS and glass walls have been added to the picture. It clearly appears that CpCl−NaSal slips much more on PDMS walls.

plate data. Tuning the surface of the channel to increase the affinity with the structured fluid allows slip effects to be avoided,[27−29] which strongly affect the measurements at low shear rates. Another solution consists of using a millimetric device to reduce the influence of the slip length, but in this case, the quantity of fluid injected during one experiment is greatly increased.

VI. Conclusions

In this work, we have implemented a viscosimeter on a microfluidic device. Following the work of Galambos et al.,[10] we have used parallel flows as a pressure sensor. We have extended this approach to complex fluids and have shown that an average shear rate with a low standard deviation can be defined. We extract the flow curve of the complex fluids from the features of the parallel flow. Various samples with viscosities ranging from 2 mPa·s to 70 Pa·s have been studied. The shear rate range is from 0.2 to 2000 s^{-1}. All experiments have been performed with less than 300 μL of sample. Our data are in good agreement with the measurements obtained in a classical cone plate rheometer. It thus seems that the hypothesis of fully developed flow holds for our systems. Further studies will deal with complex fluids involving relaxation times higher than residence times in the channel to observe the temporal evolution of the viscosity. Slip and preshear effects have been discussed. Slip effects may be reduced by tuning the nature of the channel surface. Glass devices are required to study surfactant phases in water, whereas PDMS devices seem appropriate for emulsions systems and oil phase systems. The injection of the fluids has to be improved in order to avoid shear in the tubing. We plan to add tanks at the entrance of our channels.[26] Another important advantage of our microdevice deals with the use of simple optical tools. As we visualize the sample under a microscope, it is easy to couple our device with classical measurements such as birefringence and light scattering to simultaneously obtain the rheological behavior and information of the structure of the complex fluid under shear. Soon, we plan to couple this microviscosimeter with a mixer and with optical measurements to obtain a chip that will screen various formulations of a mixture and obtain complete phase diagrams.

Acknowledgment. We gratefully acknowledge support from the Aquitaine Région. We thank A. Dodge and A. Ajdari for valuable discussions and D. Van Effenterre for his help during confocal microscopy experiments.

LA060131Z

(27) Barnes, H. A. *J. Non-Newtonian Fluid. Mech.* **1995**, *56*, 221.
(28) Lauga, E.; Brenner, M. P.; Stone, H. A. In *Handbook of Experimental Fluid Dynamics*; Foss, J., Tropea, C., Yarin, A., Eds.; Springer: New York, 2005; Chapter 15.
(29) Tretheway, D. C.; Meinhart, C. D. *Phys. Fluids* **2002**, *14*, 1070.